

Evolution of radial basic function neural network for fast restoration of distribution systems with load variations

Chao-Ming Huang^{*}, Cheng-Tao Hsieh, Yung-Shan Wang

Department of Electrical Engineering, Kun Shan University, Tainan 710, Taiwan

ARTICLE INFO

Article history:

Received 2 April 2009

Accepted 1 January 2011

Keywords:

Radial basic function
Orthogonal least-squares
Enhanced differential evolution
Service restoration
Distribution engineering

ABSTRACT

This paper proposes a new algorithm to construct the optimal radial basic function (RBF) neural network for fast restoration of distribution systems with load variations. Service restoration of distribution systems is to restore power to the blacked out but unfaulted area. Basically, it is a stressful and urgent task that must be performed by system operators. In this paper, a new algorithm which combines orthogonal least-squares (OLS) and enhanced differential evolution (EDE) methods is developed to construct the optimal RBF network that shall further achieve the fast restoration of distribution systems. The proposed scheme comprises training data creation phase and network construction phase. In the training data creation phase, a heuristic-based fuzzy inference (HBFI) method is employed to build the restoration plans under various load levels. Then an optimal RBF network is constructed by OLS and EDE algorithms in the network construction phase. Once the RBF network is constructed properly, the desired restoration plan can be produced as soon as the inputs are given. The proposed method was tested on a typical distribution system of the Taiwan Power Company (TPC). Results show that the proposed method outperforms the existing methods in terms of convergence performance and forecasting accuracy.

© 2011 Elsevier Ltd. All rights reserved.

1. Introduction

Service restoration of distribution systems is a complicated combinatorial optimization problem that often has a great number of candidate solutions to be selected by the system operators. When a fault takes place, the blackout area and the number of customers affected depend heavily on the effectiveness of service restoration algorithm. Generally, the system operators including those of TPC tend to restore the electricity power on the basis of their existing knowledge and heuristic rules. However, owing to a great number of feeder and lateral switches in a typical distribution system, it is not easy to restore an out-of-service area solely depending on the past experiences of human operators. Therefore, how to devise a fast and effective restoration plan with various load levels is of major concern in this paper.

Many researches have been devoted to coping with the problems of service restoration. Knowledge-based expert system technique [1] has been employed to incorporate the experts' experiences into the computer codes of service restoration. The disadvantage of this technique is the difficulty in designing an efficient inference engine from much of the knowledge. Combined with the past experiences of humans, the heuristic search approach [2,3] has been developed by the operators at many utilities

including those of TPC in order to reach a proper restoration plan in a short period.

Since the experts' experiences and heuristic rules are often expressed in imprecise linguistic terms, the fuzzy reasoning approach [4,5] was then proposed to achieve an efficient inference for the problem of service restoration. To deal with the problem of service restoration with many conflicting objectives, the multiobjective fuzzy reasoning approach was presented in [6,7].

In general, these techniques mentioned above can serve as a useful tool to reach a proper restoration plan for a specific load demand. However, the related inference programs need to be rerun when the system load varies. With the advantages of fast response and real-time natures, the artificial neural network (ANN) method has been used to solve the service restoration of distribution systems [8]. The ANN, however, still has the problem of slow convergence during training and the determination of network structure is problem dependent. In addition, the learning algorithm used by ANN to tune the weighting value in the network may easy to stall at the local optimal points.

To reach the goal of fast restoration of distribution systems, a systematical method which comprises training data creation phase and network construction phase is developed in this paper. In the phase one, a HBFI method [4] is employed to create the training data of restoration plans under various load levels. Then the RBF network evolved by OLS and EDE algorithms is used to train the obtained training data in the second phase. Once the RBF network is

^{*} Corresponding author.

E-mail address: h7440@ms21.hinet.net (C.-M. Huang).

constructed properly, the desired restoration plan can be obtained as soon as the inputs are given.

The RBF network consists of input, hidden, and output layer. To simplify the network, the OLS algorithm [9] is used to determine an adequate number of centers in the hidden layer. With an appropriate network structure, the EDE algorithm is then employed to tune the parameters in the network, including the position and width of RBF centers and the weights in the output layer. The proposed EDE combines DE algorithm [10] and ant system (AS) [11,12] to construct the optimal RBF networks. By simulating natural evolution process, the classical DE has the fast convergence and parallel search natures. To further enhance the global search ability of DE, an ant system was then employed to replace the *selection operation* in DE. Based on the fast convergence and global search ability, the EDE offers more probability to converge towards a global solution than the existing methods.

The rest of the paper is organized as follows. In Section 2, the fuzzy objectives are briefly reviewed. Section 3 describes the proposed method to optimize the RBF network. In Section 4, test results of the proposed method by employing the TPC systems are illustrated. Conclusions are given in Section 5.

2. Fuzzy objectives

To facilitate the description of service restoration, a simple structure of TPC distribution system, as shown in Fig. 1, is introduced. It is observed that two outgoing feeders are designed to be backed up for each other through a normally-open tie-switch. Each feeder radially supplies several lateral lines to the customers. In addition, each lateral load is backed up by a supporting lateral from other feeders.

Assume that a fault takes place at point *J* on feeder F1. Circuit breaker CB1 is tripped following the fault, which leaves all lateral loads connected to F1 out-of-service. As soon as the fault location is identified and isolated, the task of service restoration is to operate the tie-switch of supporting feeder as well as the supporting lateral switches by the HBF1 method. To achieve an effective

inference through the fuzzy rules for solving the multi-objective service restoration problem, a set of fuzzy variables should be assigned first. In this paper, we focus the objectives of restoration plan on following concerns [4]: (i) restore as much load within the out-of-service area as possible, (ii) operate minimal number of switches, and (iii) devices do not overload too much, if they must be. The other objective such as maintaining radial system structure is considered as system constraint. Definitions below are the fuzzy objectives and their associated membership functions.

2.1. Loads restored objective

The first objective considered in this paper is to restore as much load within the out-of-service area as possible. As depicted in Fig. 2a, the associated membership function is denoted as

$$\mu_1 = \begin{cases} 1, & \text{if } R_L \geq R_{LA} \\ R_L/R_{LA}, & \text{if } 0 < R_L < R_{LA} \\ 0, & \text{if } R_L = 0 \end{cases} \quad (1)$$

where R_L represents the amount of loads actually restored and R_{LA} means the amount of total lateral loads in the out-of-service area.

2.2. Switches operated objective

The second objective is to operate minimal number of switches. As shown in Fig. 2b, the associated membership function can be expressed as

$$\mu_2 = \begin{cases} 1, & \text{if } S_W \leq \underline{S}_W \\ 1 - \frac{S_W - \underline{S}_W}{\bar{S}_W - \underline{S}_W}, & \text{if } \underline{S}_W < S_W < \bar{S}_W \\ 0, & \text{if } S_W \geq \bar{S}_W \end{cases} \quad (2)$$

where S_W is the total number of switches operated, \underline{S}_W and \bar{S}_W are the possible minimal and maximal number of switching operations, respectively.

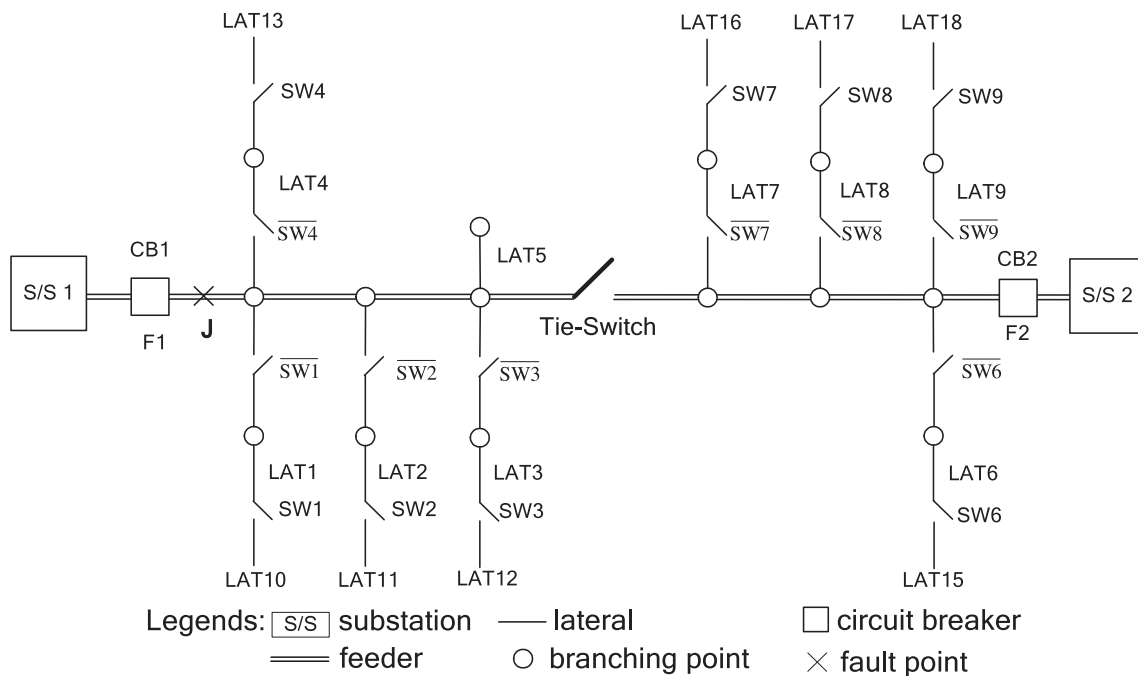


Fig. 1. A simple structure of TPC distribution system.

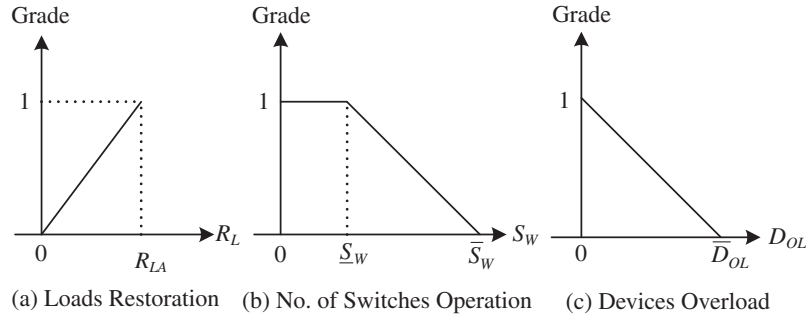


Fig. 2. The membership functions of the three objectives.

2.3. Devices overloaded objective

Since a light overload is rather common in daily operation of TPC, the associated membership function of devices overload, including supporting feeders and laterals, is depicted in Fig. 2c which can be expressed as

$$\mu_3 = \begin{cases} 1, & \text{if } D_{OL} = 0 \\ 1 - \frac{D_{OL}}{\bar{D}_{OL}}, & \text{if } 0 < D_{OL} < \bar{D}_{OL} \\ 0, & \text{if } D_{OL} \geq \bar{D}_{OL} \end{cases} \quad (3)$$

where D_{OL} represents the amount of overload for one particular device (feeder or lateral), \bar{D}_{OL} is the maximal allowable overload (in Amperes). If several devices are overloaded, including supporting feeders and supporting laterals, the resulted membership function is the one that is obtained by the AND-operation of all the corresponding membership functions.

Based on the fuzzy objective as well as their corresponding membership functions described above, the weighted-sum strategy is employed to determine the fuzzy objective value of the i th feasible solution as follows.

$$\text{Max}_{i \in \Psi} \tilde{\mu}_i = \sum_{k=1}^3 w_k \times \mu_k \quad (4)$$

where Ψ denotes the set of feasible solutions on each optimization process and w_k is the weighting value of the k th objective. The optimal decision is the one with the largest fuzzy objective value in the solution domain. Note that the weighting value w_k in (4) is determined by the system operators. In this paper, the analytical hierarchy process (AHP) method [13] is used to help the operators obtain the weighting value of each objective.

When the fuzzy objectives have been defined, the HBFI method is then employed to create the training data of restoration plans under various load levels. A clear description of the general HBFI method can be found in [4]. Due to the limit of space, it is not described in this paper.

3. Construction of optimal RBF network

When the training pairs of restoration plans under various load levels have been set up by the HBFI method, an RBF network is then employed to train the input/output data sets. Once the training data sets are learned properly, the desired restoration plan can be automatically produced as soon as the inputs are given. In this paper, a novel technique that combines OLS and EDE algorithms is adopted to construct the optimal RBF network. Details of the proposed method to optimize RBF network are stated in the subsections that follow.

3.1. The RBF network

The RBF network consists of three layers: an input layer, a single layer of nonlinear transfer neurons, and an output layer. Fig. 3 shows the architecture of the RBF network. Based on the supervised learning method, the input and output layers are presented with training pairs, each consisting of a vector from an input space and a desired network response. Through a defined learning algorithm, the error between the actual and desired response is minimized relative to some optimization criterions.

As shown in Fig. 3, the i th output node of the RBF network can be expressed as

$$Y_i = \sum_{k=1}^s \phi_k(\|\mathbf{x} - \mathbf{c}_k\|) \times w_{ik}, \quad i = 1, 2, \dots, m \quad (5)$$

where $\mathbf{x} \in \mathfrak{R}^{n \times 1}$ is an input vector, $\mathbf{c}_k \in \mathfrak{R}^{n \times 1}$ are the RBF centers in the input vector space, $\|\bullet\|_2$ denotes the Euclidean norm, $\phi_k(x) (= \exp(-x^2/\sigma^2))$ is the Gaussian function of the k th center with spread parameter σ , and $w_{ik} \in \mathfrak{R}^{m \times s}$ are the weights between hidden and output layers.

From (5) we see that there are four sets of parameters governing the mapping properties of the network: the number of centers in the hidden layer, the position of RBF centers, the width of RBFs, and the weights in the output layer. In general, a sufficient number of centers are randomly chosen as a subset of the input space according to the probability density function of the training data. Then the stochastic gradient (SG) approach [9] is used to tune the weights in the output layer. The disadvantage of this method is that it is very difficult to quantify how many numbers of center should be adequate to cover the input vector space. Furthermore,

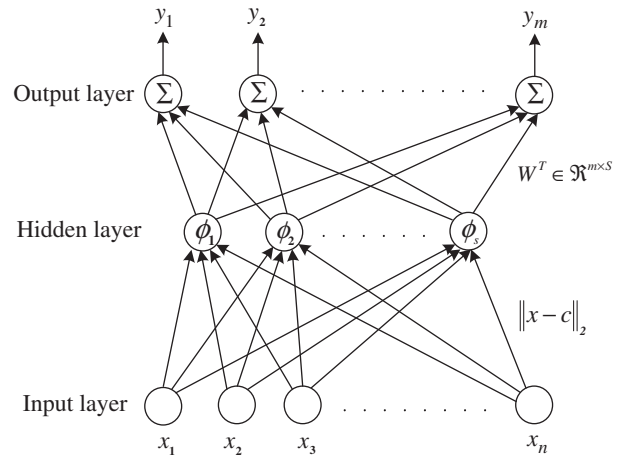


Fig. 3. The architecture of RBF network.

the training algorithm is prone to fall into the local minimum. In this paper, the OLS algorithm is employed to determine the number of RBF centers, the remainders are then tuned by using the EDE algorithm.

3.2. Network simplification using OLS algorithm

The OLS combines the Gram-Schmidt orthogonalization process with the forward regression method to simplify the RBF network. As shown in (5), the outputs of the RBF network can be viewed as a regression model as follows.

$$Y = W^T \Phi + E \quad (6)$$

where $Y \in \mathfrak{R}^{m \times 1}$ is an output vector; $W^T \in \mathfrak{R}^{m \times S}$ is a weighting matrix; $\Phi \in \mathfrak{R}^{S \times 1}$ is a linear regression vector; and $E \in \mathfrak{R}^{m \times 1}$ is the vector of regression errors between the desired and actual network outputs.

The linear regression vector Φ can be decomposed into the product of a set of orthogonal basis vectors D and an upper triangular matrix A as follows.

$$\Phi = DA = \begin{bmatrix} d_1 & d_2 & \cdots & d_S \end{bmatrix} \begin{bmatrix} 1 & a_{12} & \cdots & a_{1S} \\ 0 & 1 & \cdots & a_{2S} \\ \vdots & \vdots & \ddots & \vdots \\ 0 & 0 & \cdots & 1 \end{bmatrix} \quad (7)$$

where $D^T D = H = \text{diag}(h_1, h_2, \dots, h_S)$, and $h_i = d_i^T d_i \sum_{k=1}^S d_{ik}^2$ is a diagonal element of matrix H .

Aggregating (6) and (7), the desired network outputs can be rewritten as

$$Y = DAW + E = DG + E \quad (8)$$

where $G = AW$. Since the Gram-Schmidt orthogonalization ensures the orthogonality between E and DG , we have

$$Y^T Y = G^T D^T D G + E^T E = \sum_{k=1}^S h_k g_k^2 + E^T E \quad (9)$$

where the term $\sum h_k g_k^2$ represents the portion of the energy explained by the regression and g_k is a regression vector.

As shown in (9), each term in the summation on the right side represents an increment in the energy due to the inclusion of the k th center or regression vector. Therefore, a criterion to select an adequate number of RBF centers can be defined as follows.

$$E_{RR}^k = \frac{h_k g_k^2}{Y^T Y} \quad (10)$$

where E_{RR}^k represents an index of error reduction ratio due to the use of the k th RBF centers in a forward regression manner. At every regression step, an adequate RBF center is selected so that the value of E_{RR}^k is maximal.

As described above, the scheme using OLS to select an adequate number of RBF centers can be summarized below.

Step 1: Let $q = 1$. Compute the error reduction ratio of the i th center as

$$E_{RR,1}^i = \frac{h_i g_i^2}{Y^T Y}, \quad (1 \leq i \leq n) \quad (11)$$

Find

$$E_{RR,1}^{i_q} = \max \{ E_{RR,1}^i, 1 \leq i \leq n \} \quad (12)$$

where n is the number of the training input. Eq. (11) represents a ratio of the portion of the energy explained by the regression to

the square of the desired network outputs. In this step, select $c_1 = c_{i_q}$, c_1 is the first selected center.

Step k: Let $q \geq 2$. Compute

$$E_{RR,q}^i = \frac{h_i g_i^2}{Y^T Y}, \quad (1 \leq i \leq n, i \neq i_1, i \neq i_2, \dots, i \neq i_{q-1}) \quad (13)$$

Find

$$E_{RR,q}^{i_q} = \max \{ E_{RR,q}^i, 1 \leq i \leq n, i \neq i_1, i \neq i_2, \dots, i \neq i_{q-1} \} \quad (14)$$

and select $c_q = c_{i_q}$.

Step k+1: Repeat step k . The regression is stopped at step $S1$ when

$$1 - \sum_{i=1}^{S_1} E_{RR,q}^i < \varepsilon \quad (15)$$

where $0 < \varepsilon < 1$ is a tolerance value determined by the operators.

3.3. The proposed EDE algorithm

3.3.1. The differential evolution algorithm

Based on the basic evolutionary strategies, DE achieves the fittest individual after repeated initialization, mutation, recombination, and selection operations. The general scheme of the DE algorithm is described as follows.

3.3.1.1. Initialization. Let $p_i = [p_{i1}, p_{i2}, \dots, p_{iM}]$ be a trial vector representing the i th individual ($i = 1, 2, \dots, P$) of the population to be evolved, where P is the population size and M is the dimension of each individual. The elements in vector p_i represent the decision variables (genes) which are randomly generated as follows.

$$p_{ij} = p_{ij,\min} + \beta \times (p_{ij,\max} - p_{ij,\min}), \quad j = 1, 2, \dots, M \quad (16)$$

where p_{ij} represents the j th gene of the i th individual, $p_{ij,\min}$ and $p_{ij,\max}$ mean the lower and upper bounds of p_{ij} , respectively, and β represents the uniform random number between 0 and 1.

3.3.1.2. Mutation. The mutation operation is performed by adding a differential vector to the parent individual as follows.

$$p'_i = p_i + f_m \times (p_{i_a} - p_{i_b}) \quad (17)$$

where p_{i_a} and p_{i_b} are the randomly selected individuals in the parent population, $(p_{i_a} - p_{i_b})$ is a differential vector, and $f_m \in [0, 1]$ represents the mutation factor.

3.3.1.3. Recombination. In essence, the mutant individual in (17) is a noisy replica of p_i . When the population diversity is small, the candidate individuals will rapidly gather together so that the individuals cannot be further improved. In order to extend the local diversity of the mutant individuals, a recombination operation is introduced as follows:

$$p'_{ij} = \begin{cases} p_{ij}, & \text{if } \text{rand}_{ij} > R_r \\ p'_{ij}, & \text{if } \text{rand}_{ij} \leq R_r \end{cases} \quad (18)$$

where p_{ij} is the j th gene of the i th individual before mutation, p'_{ij} represents the j th gene of the i th offspring individual after mutation, rand_{ij} is a random number with normal distribution, and $R_r \in [0, 1]$ is a recombination factor. Eq. (18) indicates that each gene of the i th individual is reproduced from the current gene p_{ij} or the mutant gene p'_{ij} .

3.3.1.4. Selection. Each offspring individual must compete against its parent individual based on the fitness values as follows:

$$p'_i(t+1) = \begin{cases} p_i(t+1), & \text{if } f(p_i(t+1)) < f(p_i(t)) \\ p_i(t) & \text{otherwise} \end{cases} \quad (19)$$

where $f(p_i(t+1))$ and $f(p_i(t))$ represent the fitness values of the i th individual at $t+1$ and t iteration, respectively. As shown in (19), it is observed that any parent individual will be replaced by its offspring individual if the fitness value of the parent individual is worse than that of its offspring individual. It means that the optimal decision is the one with the lowest fitness value in the solution domain.

3.3.2. The ant system

The DE employs one-to-one competition to retain its offspring that gives rise to a faster convergence rate. This faster convergence may lead to a higher probability of obtaining a local optimum because the diversity of the population descends faster during the optimization process. To increase the global search ability, an ant system is employed to replace the *selection operation* in DE.

The ant system (AS) was first applied to the traveling salesman problem [11,12]. Informally, ants prefer to move to cities which are connected by short distance with a high amount of pheromone. However, the cities with short distance and high pheromone are not absolutely selected by ants. Each ant generates a complete tour by choosing the cities according to a probabilistic state transition rule as follows.

$$\text{Pr}_i(t) = \frac{[\tau_i(t)]^\gamma [\tilde{\mu}_i]^\psi}{\sum_{i=1}^P [\tau_i(t)]^\gamma [\tilde{\mu}_i]^\psi} \quad (20)$$

where $\tau_i(t)$ is the pheromone concentration of the i th ant at t th iteration, $\tilde{\mu}_i$ is the fuzzy objective value as denoted in (4), γ and ψ are the weighting constants of both pheromone and fuzzy objective value, respectively.

In addition, the pheromone concentration is updated according to the following formula:

$$\tau_i(t+1) = \rho\tau_i(t) + \Delta\tau_i \quad (21)$$

where

$$\Delta\tau_i = \begin{cases} \frac{q}{d_i}, & \text{if } i\text{th ant is better so far} \\ 0, & \text{otherwise} \end{cases} \quad (22)$$

ρ is a pheromone decay parameter ($0 < \rho < 1$), q is a constant, and d_i is the Euclidean distance. In this paper, d_i represents the fitness value as denoted in (19).

3.4. Parameters adjustment using EDE

The EDE algorithm for tuning the position and width of RBF centers and the weights between hidden and output layers can be described in the following steps:

- *Step 1:* Randomly generate the initial parent trial vector p_i , $p_i = [p_{i1}, p_{i2}, p_{i3}]$, where p_{i1} and p_{i2} represent the possible solutions of position and width of RBF centers, respectively, and p_{i3} represents the weighting vector between hidden and output layers. The elements of p_{i1} , p_{i2} , and the weighting vector p_{i3} can be obtained by using (16).
- *Step 2:* Evaluate the fitness value of each parent individual. In this paper, the criterion of mean squared error (MSE) function defined below is adopted to stand for the fitness value of the RBF network.

$$\text{MSE} = \frac{1}{m} \sum_{i=1}^m [y_i - \hat{y}_i]^2 \quad (23)$$

where y_i is the i th computed output of the RBF network by using (4), \hat{y}_i is the corresponding actual output, and m is the number of network output nodes.

- *Step 3:* Execute the mutation and recombination operations according to the mutation factor f_m and recombination factor R_r , as described in (17) and (18), respectively.
- *Step 4:* Proceed to calculate the fitness value of each offspring individual by using (23).
- *Step 5:* Perform the selection operation by using AS method described in (20) to retain P sets of individual in the population.
- *Step 6:* Repeat steps 3–5 until the desired MSE value is obtained. The solution with the lowest fitness value is chosen as the best individual in the RBF network that shall further be applied to the fast restoration of distribution systems.

4. Numerical results

To demonstrate the performance of the proposed method, a typical distribution system within the service area of Taipei West District Office of TPC [4], as shown in Fig. 4, is employed in this paper. The fast restoration scheme was implemented using the commercial MATLAB package. For comparison, the ANN [8] and the RBF network evolved by stochastic gradient (GS) [9] and genetic algorithm (GA) [14] methods are also tested using the same database.

As described previously, the proposed fast restoration system comprises training data creation phase and network construction phase. For clarity, they are implemented individually in the following subsections.

4.1. Training data creation

In the training data creation phase, a HBF1 method is employed to achieve the task of service restoration under various load levels. As shown in Fig. 4, suppose that one fault took place at point J located at feeder YD28. The circuit breaker CB2 was then tripped and the faulted zone was isolated that left lateral loads from LAT1 to LAT9 out-of-service. Since LAT9 is not equipped with supporting lateral, it must be supplied power from the supporting feeder YE29. In this phase, our goal is to set up the restoration plans for restoring these lateral loads under various load levels.

As shown in Fig. 2, three objectives including loads restoration, switches operation, and devices overload are considered. Since there are nine lateral loads to be restored, the parameter R_{LA} , as shown in Fig. 2a, is set at 9. The operation switches of S_W and \bar{S}_W depicted in Fig. 2b are set at 3 and 17, respectively. In addition, the rated capacities for feeder and laterals are 450 A and 100 A, respectively. But in the daily operation of TPC, overloads of 10% and 20%, for feeders and laterals, respectively, are allowed. Therefore, the parameters of \bar{D}_{OL} depicted in Fig. 2c for feeder and lateral are set at 45 A and 20 A, respectively. Besides, the weighting values of these three objectives (loads restoration, switches operation, and devices overload) obtained by AHP method are 0.5396, 0.2970, and 0.1634, respectively.

The input data to the network can be defined as follows.

$$\mathbf{x} = [x_1, x_2, \dots, x_9 | x_{10}] \quad (24)$$

where x_1 – x_9 are the lateral loads (in ampere) from LAT1 to LAT9 and x_{10} represents the capacity margin of the supporting feeder. The elements of the vector \mathbf{x} can be normalized according to the following equation:

$$x'_i = 0.1 + 0.8 \times \left(\frac{x_i - x_{i,\min}}{x_{i,\max} - x_{i,\min}} \right) \quad (25)$$

where $x_{i,\min}$ and $x_{i,\max}$ are the minimal and maximal value of x_i ($i = 1, 2, \dots, 10$), respectively. The outputs of the training network are defined as follows.

$$\mathbf{Y} = [y_1, y_2, \dots, y_9 | y_{10}]^T \quad (26)$$

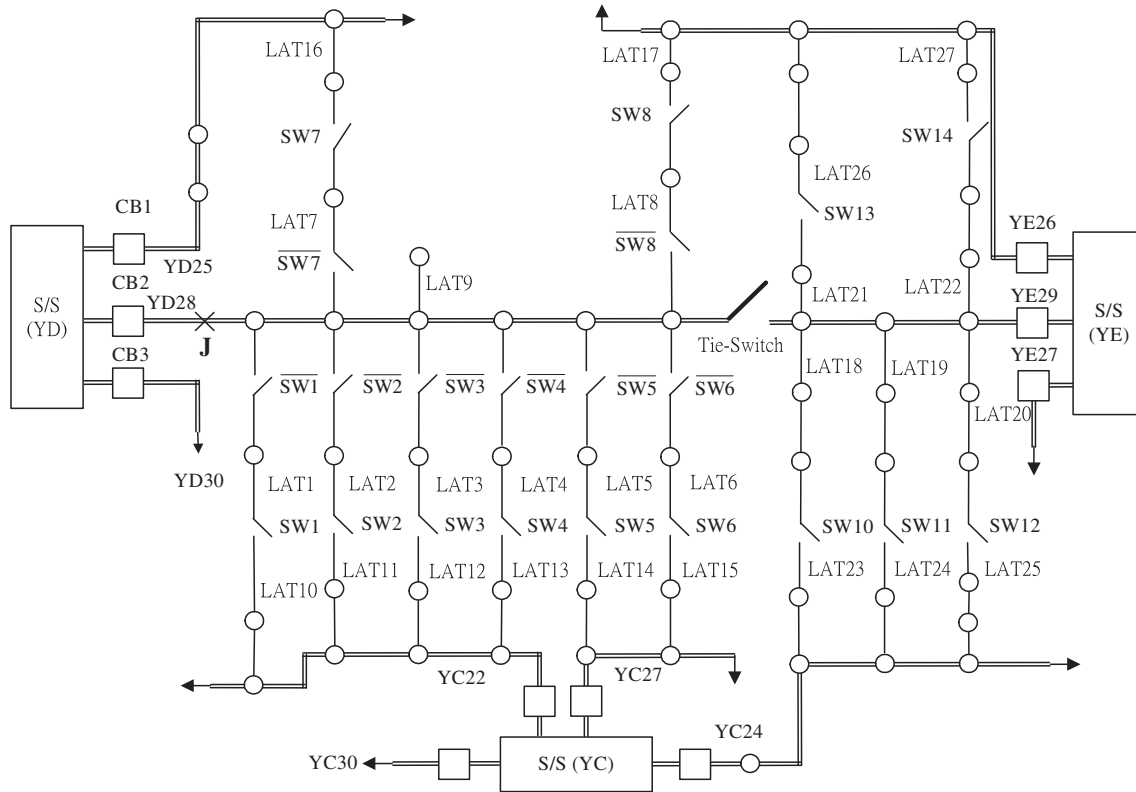


Fig. 4. A typical TPC distribution system.

where $y_i = 0$ ($i = 1, 2, \dots, 10$) if the i th normally-open lateral (or feeder) switch is open, whereas $y_i = 1$ if the i th normally-open lateral (or feeder) switch is closed. Note that $y_i = 1$ ($i = 1, 2, \dots, 9$) represents the i th lateral load can be restored by the supporting lateral.

Table 1 shows the basic data of pre-faulted lateral loads and feeders. The values in the table represent the rated capacity of current prior to the outage. Because there are too many lines and components in a distribution system, it is not economically justifiable to install real-time monitoring and control devices everywhere along feeders and laterals. Even when the distribution automation project in TPC is completed, only feeder loads will be monitored. Due to the lack of real-time information on the distribution system, only the total feeder current recorded at substations is available. Therefore, the other important issues such as maintaining frequency and voltage magnitude constraints will not be investigated in this paper.

Based on the HBFI method, the restoration plans are obtained by varying different load levels. These load levels are defined in such a way that they should cover all of the possible load conditions. In this paper, a total of 200 samples are created under different load levels, where 150 samples are used for training and the other 50 samples are provided for testing.

4.2. Network construction

In the network construction phase, some parameters should be set first. The ANN method had a four-layer architecture (ten input

nodes, 50 hidden nodes in the second layer, 25 hidden nodes in the third layer, and ten output nodes), a learning rate of 0.05, a momentum constant of 0.85, and was trained by 5000 iterations. For the RBF network, an OLS algorithm is used to simplify the RBF network. Fig. 5 depicts the trend of MSE versus the number of RBF centers. As noted, when the number of centers rises, the MSE value decreases progressively. In this case, 101 centers are chosen to perform the exact mapping of all 150 centers, as given in Fig. 6. With the same network structure, the proposed EDE and the other methods are employed to tune the network parameters, including the position and width of RBF centers and the weights in the output layer.

As described above, the RBF network contains ten input nodes, 101 hidden nodes, and ten output nodes. The mutation factor f_m and recombination factor R_r for EDE are set at 0.05 and 0.80, respectively. The same values are set for the GA method.

Fig. 7 depicts the optimization processes of the best fitness value obtained by different optimization methods. After 19 iterations, the proposed EDE converges toward the best one, while the GA and ANN methods need about 45 and 215 iterations, respectively. Note that the conventional SG method cannot reach the desired fitness value after 5000 iterations. The figure reveals that the proposed EDE converges faster than the other methods.

Table 2 shows the comparison results of different methods. The column of accuracy for 150 training data indicates that the 150 training samples are used to verify the constructed network,

Table 1 Basic data of pre-faulted lateral loads and feeders.

Laterals (Ampere, A)	LAT1 35	LAT245	LAT331	LAT417	LAT5 54	LAT6 61	LAT7 51	LAT8 25	LAT9 20
Supporting lateral (Ampere, A)	LAT10 51	LAT11 39	LAT12 46	LAT13 37	LAT14 34	LAT15 38	LAT16 23	LAT17 80	None
Feeders (Ampere, A)	YD28 346	YD25 240	YC22 220	YC27 260	YE26 250	YE29 175			

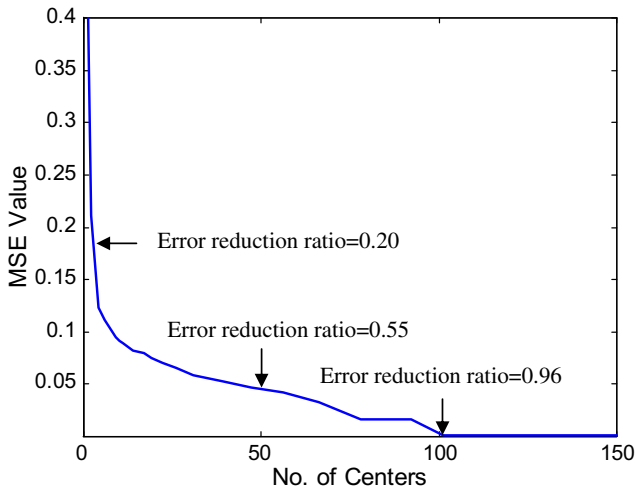
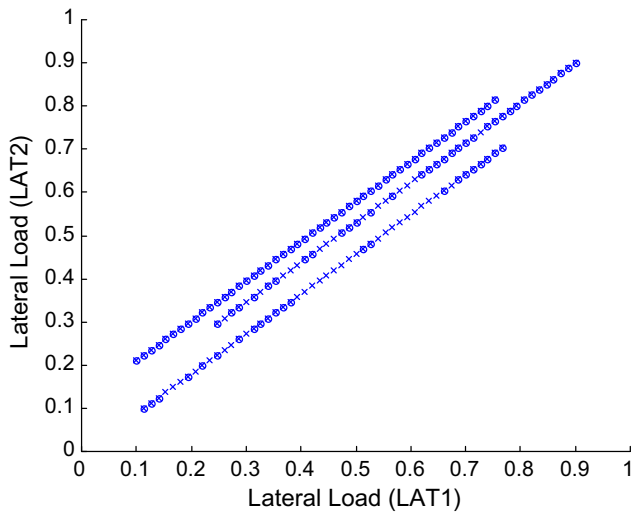


Fig. 5. Trend of MSE versus the number of RBF centers.



(x : Initial RBF centers ; o : Selected RBF centers)

Fig. 6. Distribution of initial (150) and selected 101 RBF centers.

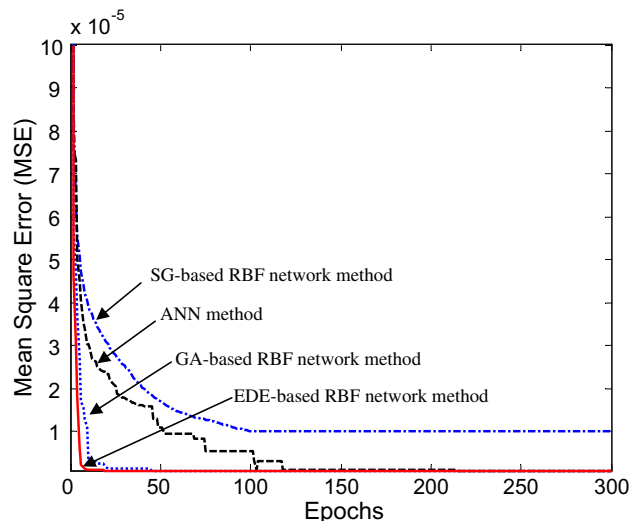


Fig. 7. Optimization processes of different methods.

Table 2
Comparison results of different methods.

Methods	Accuracy for 150 training data (%)	Accuracy for 50 testing data (%)
ANN ^a method	100	84
SG ^b -based RBF network	76.67	74
GA ^c -based RBF network	100	90
EDE ^d -based RBF network	100	98

^a Artificial neural network.
^b Stochastic gradient.
^c Genetic algorithm.
^d Enhanced differential evolution.

Table 3
Training time for historical training data (100 trials with different random numbers).

Method	Ave. (s)	Min. (s)	Max. (s)	Max.–Min. (s)
ANN method	90.75	84.25	93.66	9.41
GA-based RBF network	38.50	36.60	39.50	2.90
EDE-based RBF network	9.05	9.00	9.12	0.12

Note: The SG-based RBF network method cannot converge after 5000 iterations.

whereas the column of accuracy for 50 testing data represents that a total of 50 additional samples are employed to assess the forecasting capability of diverse methods. To show the convergence performance of different methods, 100 trials with diverse random numbers are executed. Table 3 shows the historical training time obtained by different methods. Obtained from Tables 2 and 3, it is observed that the proposed EDE can provide better characteristics in terms of forecasting capability and convergence performance.

Once the networks are trained properly, the best restoration plan can be obtained as soon as the inputs are given. Table 4 shows the restoration plans obtained by different input vectors. As shown in case I, the advantage of less operation switch is achieved by the proposed EDE at the cost of overload on the supporting feeder of YE29 (8A). In case II, the same fuzzy objective value is obtained by the proposed and other methods. In case III, the ANN reaches the restoration plan with the cost of nine operation switches, while the GA and proposed EDE need only seven operation switches. In addition, a larger overload is taken plan on the supporting feeder of YE29 (11A) by the GA method.

5. Conclusions

A new algorithm which combines OLS and EDE algorithms has been developed to construct the optimal RBF network for fast restoration of distribution systems under various load levels. Four main contributions are provided as described below.

The proposed approach provides an effective method to simplify the structure of the RBF network.

With the enhanced evolution strategies, the proposed EDE provides more efficient fitting and forecasting capabilities than SG and GA methods based on the same network structure.

The proposed approach can cope with the restoration problem with load variations.

After the RBF network is constructed properly, the desired outputs of restoration plan can be produced extremely fast as soon as the inputs are given.

Although this paper only provides the results of restoration plan with the fault that takes place on feeder yd28, the proposed

Table 4
Restoration plans obtained by different input vectors.

Input vector (x)	Restoration plan				
	Method	Operated switches	Load unrestored	Overload	Fuzzy objective value
Case I: $x = [42, 52, 38, 24, 61, 68, 58, 32, 27, 1275]^T$	ANN	Tie-Switch, SW3, $\overline{SW3}$, SW5, $\overline{SW5}$, SW7, $\overline{SW7}$	None	None	0.9151
	GA	Tie-Switch, SW4, $\overline{SW4}$, SW5, $\overline{SW5}$, SW7, $\overline{SW7}$	None	None	0.9151
	EDE	Tie-Switch, SW5, $\overline{SW5}$, SW7, $\overline{SW7}$	None	YE29(8A)	0.9285
Case II: $x = [32, 42, 28, 14, 51, 58, 48, 22, 17, 1275]^T$	ANN	Tie-Switch, SW5, $\overline{SW5}$	None	None	1.0000
	GA	Tie-Switch, SW6, $\overline{SW6}$	None	None	1.0000
	EDE	Tie-Switch, SW6, $\overline{SW6}$	None	None	1.0000
Case III: $x = [48, 58, 44, 30, 67, 74, 64, 38, 33, 1275]^T$	ANN	Tie-Switch, SW1, $\overline{SW1}$, SW2, $\overline{SW2}$, SW3, $\overline{SW3}$, SW4, $\overline{SW4}$	None	YE29(1A)	0.8691
	GA	Tie-Switch, SW1, $\overline{SW2}$, SW2, $\overline{SW2}$, SW7, $\overline{SW7}$	None	YE29(11A)	0.8752
	EDE	Tie-Switch, SW2, $\overline{SW2}$, SW5, $\overline{SW5}$, SW7, $\overline{SW7}$	None	LAT14(1A)	0.9151

method is also adequate for dealing with the faults that occur on the other locations.

Acknowledgements

The authors would like to thank Mr. Fu-Zu Wang, Senior Engineer of Taiwan Power Company, for his providing the valuable data used in this paper. Financial supports from the National Science Council, Taiwan, R.O.C under the Grant No. NSC 95-2221-E-168-044 are acknowledged.

References

- [1] Liu CC, Lee SJ, Venkata SS. An expert system operational aid for restoration and loss reduction of distribution system. *IEEE Trans Power Syst* 1998;3(3): 619–26.
- [2] Hsu YY, Huang HM, Kuo HC, Peng SK, Chang CW, Chang KJ, et al. Distribution system service restoration using a heuristic search approach. *IEEE Trans Power Delivery* 1992;7(2):734–40.
- [3] Morelato AL, Monticelli A. Heuristic search approach to distribution system restoration. *IEEE Trans Power Syst* 1989;4:2235–41.
- [4] Hsu YY, Kuo HC. A heuristic based fuzzy reasoning approach for distribution system service restoration. *IEEE Trans Power Delivery* 1994;9(2):948–53.
- [5] Lin WM, Chin HC. Preventive and corrective for feeder contingencies in distribution systems with fuzzy set algorithm. *IEEE Trans Power Delivery* 1997;12(4):1711–6.
- [6] Lee SJ, Lim SI, Ahn BS. Service restoration of primary distribution systems based on fuzzy evaluation of multi-criteria. *IEEE Trans Power Syst* 1998;13(3):1156–63.
- [7] Hsiao YT, Chien CY. Enhancement of restoration service in distribution systems using a combination fuzzy-GA method. *IEEE Trans Power Syst* 2000;15(4):1394–400.
- [8] Hsu YY, Huang HM. Distribution system service restoration using the artificial neural network approach and pattern recognition method. *IEE Proc Gener Transm Distrib* 1995;142(3):251–6.
- [9] Ham FM, Kostanic I. *Principal of neurocomputing for science and engineering*. New York: McGraw-Hill; 2000.
- [10] Storn R, Price K. Differential evolution: a simple and efficient adaptive scheme for global optimization over continuous space. *Int Comput Sci Institute, Berkeley, Technique Report TR-95-012*; 1995.
- [11] Dorigo M, Maniezzo V, Colomi A. Ant system: optimization by a colony of cooperative agents. *IEEE Trans Syst, Man Cyber, Part B* 1996;26(1):29–41.
- [12] Dorigo M, Gambardella LM. Ant colony system: a cooperative learning to the traveling salesman problem. *IEEE Trans Evolut Comput* 1997;1(1):53–66.
- [13] Satty TL. *The analytical hierarchy process: planning, priority setting, resource allocation*. New York: McGraw-Hill; 1980.
- [14] Toune S, Fudo H, Genji T, Fukuyama Y, Nakanishi Y. Comparative study of modern heuristic algorithms to service restoration in distribution systems. *IEEE Trans Power Delivery* 2002;17(1):173–81.